INFLUENCE OF COMPOSITION ON ENERGY AT BREAK OF BLENDS PP + PA6

Andreea Elena MUSTEATA[1], Horia PETRESCU[2], Alina CANTARAGIU CIOROMILA[3], George-Ghiocel OJOC[4], Lorena DELEANU[5]

This paper analyzes the influence of composition on the energy at break of blends PP+PA6. There were formulated 4 blends having a mass concentration of 20%, 40%, 60 and 80% PA6, respectively and the same quantities of compatibilizing additives (5% LDPE, 7% $CaCO_3$ and 3% Polybond 3200). Fig. 1 presents the result data of load and absorbed energy versus time, till break, for the blend with 80% PA6. Charpy tests were done on ten notched samples, at a velocity of v=0.96 m/s. There were analyzed the influence of PA6 concentration on average values for maximum load and energy at break. Better results were obtained for blends with high concentration of PA6. SEM investigation pointed out failure mechanisms depending on constituents' concentration.

Keywords: polyamide 6, polypropylene, blend, Charpy test, blend morphology

1. Introduction

Polymeric blends have developed in parallel with the advance of polymers. Shortly after the generation of nitrocellulose, it was blended with nitrile rubber. The first compatible blend dates from 1928 and is that of polyvinyl chloride (PVC) with polyvinyl acetate (PVA) and its copolymers. Nowadays, polymeric alloys and blends, also their composites have over 80% (by mass) of the total polymer-based market [1], [2].

Polymer blends are attractive for specialists and end-users due to a set of better particular characteristics, such as low specific mass, strength-to-mass and stiffness-to-mass ratios, tribological properties [3], [4], resistance to aggressive environments, electrical and thermal properties, which recommend them in the

[1] PhD student, eng., Department of Mechanical Engineering "Dunărea de Jos" University of Galati, Romania, e-mail: musteata_andreea90@yahoo.com
[2] Assist. prof., PhD eng., Department of Materials Resistance, University POLITEHNICA of Bucharest, Romania, e-mail: horia.petrescu@upb.ro
[3] PhD phys., Department of Chemistry, Physics and Environment, "Dunărea de Jos" University of Galati, Romania, e-mail: Alina.Cantaragiu@ugal.ro
[4] PhD student, eng., Department of Mechanical Engineering "Dunărea de Jos" University of Galati, Romania, e-mail: george.ojoc@ugal.ro
[5] Professor, Department of Mechanical Engineering, "Dunărea de Jos" University of Galati, Romania, e-mail: lorena.deleanu@ugal.ro

field of aeronautics, shipbuilding, machine building, fine mechanics, electronics, medical equipment etc. Blends may be obtained with miscible polymers and with immiscible polymers, as it is the case of PP + PA6 blends.

Polymer blending is a versatile and economical method of producing materials meeting complex performance demands. The trend is to offer blends that may be processed and designed like any other polymer on the market; therefore, their workability must match that of simple polymers, but they offer a much wider range of performance possibilities.

The advantages of polymer blends fall into two categories: improving product performance (materials with a complex set of improved properties, at low costs) and improving their processability [5].

This paper analyzes the influence of composition on the energy at break of blends PP+PA6, data measured and calculated from Charpy tests.

2. Formulated blends and test parameters

There were formulated 4 blends having a mass concentration of 20%, 40%, 60 and 80% PA6, respectively and the same quantities of compatibilizing additives.

Polypropylene (PP) is a cheap thermoplastic polymer, with versatile applications, high purity and chemical stability. PP belongs to the category of polyolefins, thermoplastics with a widely spread properties. Its set of properties makes it suitable for a wide variety of engineering applications [6]. It offers exceptional chemical resistance at a relatively low cost. It has medium impact resistance, fair structural strength and resistance to a large range of chemicals. PP is mainly processed by injection, but also by extrusion or thermoforming [7]. Trademarks usually contain antioxidants and other additives [8], [9]. The set of properties that includes low density, high degree of crystallinity, high melting point (T_m=166 °C) and a deformation temperature under load higher than 90 °C also indicates good processability [6]. The crystallinity of the isotactic PP homopolymer has a brittle behavior at low temperatures or on impact, if the designed parts have high stress concentrators (sharp notches, holes etc.). The low temperature impact resistance of unmodified PP and the Izod impact resistance give lower values than those obtained for PE. Fragility increases in the presence of stress concentrators, especially at negative temperatures [10], [11].

For PP with additives, composites or blends, induced shear fibrillation and tip crack propagation were observed for the droplets in the matrix. The impact resistance of PP can be improved with an elastomer modifier. The rigidity of the blend decreases with increasing the elastomer content. The interpretation of mechanisms responsible for increasing the impact resistance of modified PP with elastomers is based on multiple crazing, shear flow and cavitation and micropore

formation. The elastomer particles in the PP matrix should be uniform in size and the interfacial adhesion between PP and elastomer should be good [12]. Like PA, PP accepts as elastomeric compatibilizers, such as those based on ethylene propylene (EP or EPDM) in low to medium concentrations (5% to 25 wt%). Low density polyethylene (LDPE) [13] and high-density polyethylene (HDPE) can be added to improve the stability of elastomeric particles and to improve the set of tensile and impact properties.

Polyamides have many applications due to an easy processability, good to excellent tribological behavior (low friction and wear resistance) [14], and rather high melting temperature, but they have the disadvantage of a higher cost, critical fragility to space demands and water absorption. The effects of the environment on the properties of polyamides include high sensitivity to moisture and water absorption. Increasing the crystallinity degree of polyamides influences the mechanical properties (increases hardness and wear resistance, reduces opacity and shock resistance). Copolymerization contributes to increased transparency, flexibility and reduced melting temperature.

The PP + PA6 blends have been tested for improved mechanical properties: PP induces good processability and moisture insensitivity and PA6 contributes with thermal and mechanical properties. In the recent years, their nanocomposites have also attracted the attention of the industry. As a result of nanoscale dispersions, composites show a significant mechanical improvement as compared to conventional composites. Till recently, researchers have described nanocomposites based on a unique polymer matrix. Composites based on blends of two or more polymers (binary or ternary blends) are a newer approach and nanocomposites based on PP + PA6 blends were studied [15], [16]. These may have properties in wide ranges, even for reinforced blends. Sharma [17] highlighted that PA+PP blends were introduced by DSM, Atochem and Mitsubishi (automotive industry) because they have lower water absorption than polyamide, dimensional stability (as an influence of PP), low density, low permeability of liquids and vapors, moderate impact resistance induced by PA and good resistance to alcohols and glycols. PP + PA blends are immiscible mixtures, usually with strongly asymmetrical compositions (90/10, 80/20 or 70/30), which often have larger island morphologies and lack of adhesion between phases, caused by high values of interfacial stresses between immiscible phases. If any compatibilizers are not added, the mixtures have poor mechanical properties, but better results have been recently reported, with compatibilizing additives [9], [18], [19], [20], [21]. The compatibilizers for these blends are block copolymers, with different architectures (linear, stellar, crosslinked, cyclic polymers), spherical, plaquette-like nano and micro particles [22], [23], [24], elastomers [25], [9]. Clay particles serve as effective nucleating agents that can alter the crystalline morphology of polymers, such as PA6 and PP [17].

Bai et al. [19] developed a class of blends of three phases: PP, PA6 and polyethylene-octene elastomer (POE) grafted with maleic anhydride. The mass fraction of PA6 was adjusted from 0 to 40%, in steps of 10%, and the mass fraction of POE was kept at half that of PA6. The morphology was mainly from PA6 particles dispersed in the PP matrix. The POE modifier was observed as a thin interface (less than 100 nm thick) at the PP/PA6 interface, and as isolated, but few, particles. The modulus of elasticity and the tensile strength are almost constant for PP and blends. But the Izod impact resistance greatly increases with the content of the alloying components. This effect resulted from POE cavity at interface, high shear plastic deformation and resistance of PA6 particles to crack propagation.

Laoutid et al. [26] reported that the incorporation of 5 wt% hydrophobic nanosilica in PP+PA blends (80+20 wt/wt) led to a change in mechanical properties and a reduction in the size of dispersed droplets due to the preferential migration of silica nanoparticles at the interface between PP and PA or PC, which led to the formation of an anti-coalescence barrier around the isolated droplets.

Blends with elastomer particles, dispersed in the PA matrix, began to be used [20], [27]. New trademarks also contain short fiberglass, glass beads, clay and/or mineral powders. The applications of these blends are in various fields: sports and holiday equipment, medicine, automotive industry. Although immiscible, there is a degree of compatibility between EP elastomers and PP matrix, which leads to low interfacial tension and satisfactory interfacial adhesion [10].

Beuguel et al. [24] studied the influence of component concentration on the morphology and rheological properties of PP/PA12/mineral or synthetic clay blends. A more viscous PP matrix produces a more developed interface by slowing the migration of clay particles from the PP matrix into the PA12 nodules.

Due to the semi-crystalline nature, thermoplastics have a high shrinkage during cooling and this can cause problems in achieving the accuracy of the parts injected into the mold. Mineral additives reduce the overall shrinkage, but if the particles are not isotropic, they can cause a differentiated shrinkage, leading to dimensional and shape instability [28], [8]. Flattened agents, of sheet type, are generally more efficient, giving the best values in reducing shrinkage, while maintaining properties suitable for the application [29].

Ground calcium carbonate is added in thermoplastics, especially in PVC, but also in PP and polyamides. The advantages are: low production price, small particle aspect ratio (towards spherical), high purity, improvement by cheap fatty acids. Calcium carbonate may have crystalline changes, but calcite is the most commonly used form in polymers. [30]. Most natural calcium carbonates, used in thermoplastics, are treated with fatty acids (for not absorbing water). In order to

obtain good physical and mechanical characteristics, the uniform dispersion of clays and minerals is, sometimes, a difficult requirement to achieve.

Wang et al. [31] added organic clay (montmorillonite, 1 wt% and 4 wt%) and EPDM-g-MA (5 wt% to 40 wt%) to improve impact resistance and PA6 rigidity. The effects of clay on the morphology of the PA6/EPDM-g-MA blend were: weakening of interphase adhesion between PA6 and EPDM-g-MA particles led to the increase of elastomer particles at low concentrations of elastomer and clay, preventing coalescence between elastomer domains and reducing the size of elastomer particles in conditions of high concentration for elastomer and clay, widening the brittle-ductile transition range.

The compatibilization strategy of immiscible polymers, such as PP and PA, involves one or more additions [10], [32], [33]:

- a small amount of a third component in the polymeric blend, miscible with both basic polymers,
- a copolymer with a miscible terminal group with one phase or a polymer and the other terminal group with the other phase or the other polymer,
- a large amount of coating-type copolymer, called impact modifier, because it improves impact qualities,
- a reactive compound, which alters at least some macromolecules and, thus, develops a local miscibility,
- additives having mechanical and/or chemical influence on the blend etc.

The family of polymeric blends used for this study consists of polyamide 6, polypropylene, low density polyethylene (LDPE), calcium carbonate and a Polybond 3200 adhesive, in the concentrations as shown in Table 1.

Table 1

Recipes for the blends

Material code	Concentration [wt%]				
	PA6	**PP**	**LDPE**	**$CaCO_3$**	**Polybond 3200**
PP	-	100	-	-	-
A	20	65	5	7	3
B	40	45	5	7	3
C	60	25	5	7	3
D	80	5	5	7	3
PA6	100	-	-	-	-

In PA + PP blend recipes, interfacial interactions and their morphology with more rigid particles, partially encapsulated in an elastomeric phase in the basic matrix are the key to good results for these blends.

There is difficult to predict the influence of constituents and their concentrations on mechanical properties and testing on specimens or actual

components is the only way to have reliable data on the behavior of these materials, and to use them in design. Simulation could help to predict material behavior, but the engineers have to introduce adequate constitutive model for the material that could be reliably used in simulating the behavior of a more complex component than a test specimen [34].

The recipes were established by mutual agreement with Monofil, Săvineşti, who also processed the blends, by injection molding in parallelipipedic shape, theV-notch being cut with dedicated cutter for Charpy tests.

Pre-mixtures of PA6, PP, LDPE and Polybond 3200 granules are performed in a high speed mixer, with a capacity of 200 l, mixing speed 475/950 rpm, provided with a heating system with electric resistances of 11 kW and discharge system. Pre-mixing of components in a mixer before introducing in the extruder is necessary because they have different densities and, implicitly, a high tendency of stratifying on density if they are not pre-mixed. Thus, a higher degree of component dispersion is realized. Mixtures of polymers and additives from the high speed mixer will be placed in a drying hopper, at a temperature of 80-100°C. The pre-mixtures from the drying hopper are automatically loaded into the primary dosing system. The primary dispenser has the following technical data: dosing flow = 150 kg/h, dosing system = with double screw, dosing speed = max100 rpm; feed hopper volume = 150 l. Fig. 1 suggest the flow chart of the laboratory technology.

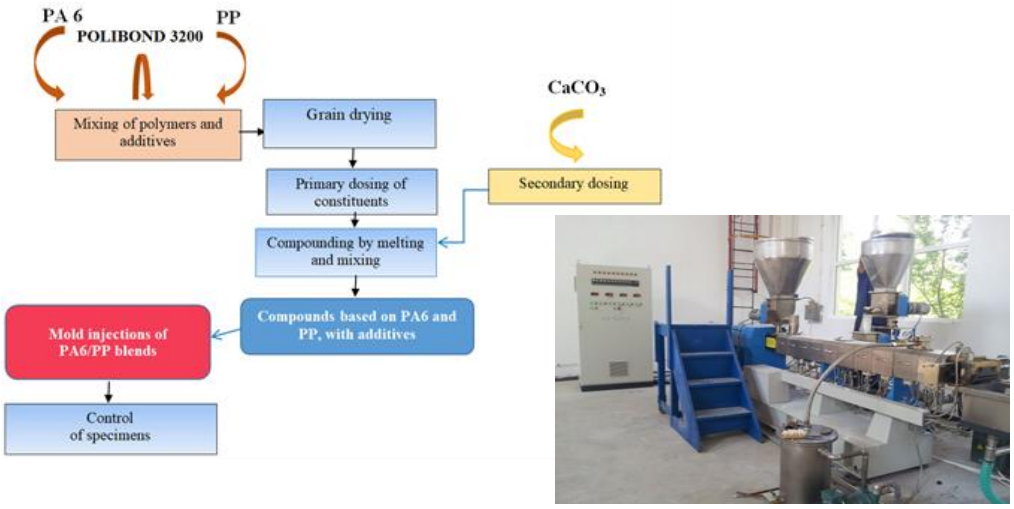

Fig. 1. The technological flow of obtaining the first class of polymeric blends, based on PA6 and PP [13] (right - EC 52 double screw granulator extruder (SC Monofil Săvineşti SA)

Plastics may differently behave depending on temperature and could exhibit a change in impact properties, from ductile to brittle, which must be evaluated when the polymeric material is introduced in an assembly [35]. Even after 100

years, Charpy's impact test procedures take place similarly. The tests for this study were performed after consulting the standards: SR EN ISO 179-1: 2010 Plastics. Determination of Charpy shock characteristics. Part 1: Non-instrumental shock test, and SR EN ISO 179-2: 2020 Plastics. Determination of Charpy shock properties. Part 2: Instrumental shock test. At the end of the testing campaign for this paper, the 2002 version of the last was in force.

Table 2

Technological parameters

Parameter	**Musteață**	**Ahn** [36]
Machine	**Extruder machine type EC52 with double screw with simultaneous rotation, diameter 51.4 mm**	Haake extruder with double screw with 30 mm diameter, wheel 26 mm and a length of 305 mm.
Processing temperature, °C	**130-150** **240-260 (PP: 170...190)** **220-230 (PP: 170...180)**	240 280 (injection nozzle)
Rotational speed, rpm		280
Power supply flow		980 g/h
Mold temperature, °C		80
Injection pressure	**50...60 bar**	70 bar
Maintenance pressure	**20 bar**	35 bar
Maintenance pressure time in mold for cooling, s		9.0

The tests were performed on the impact test machine CEAST 9340, in the materials strength laboratory at "Politehnica" University of Bucharest. Unlike pendulum equipment, it uses a pneumatic cylinder to have the desired velocity of the striker, which has a rectilinear motion, the space required being better managed than in the case of pendulum systems. According to the standard SR ISO 179, ten tests were selected for each material to be typical (tests with extreme values were eliminated). A hemispherical impactor was used, with a speed of 0.96 m/s and the mass of the impactor has 3.219 kg. Fig. 2 shows the specimen geometry and Fig. 3 the impactor geometry.

The impact strength of the specimen is calculated with the formula

$$R_{impact} = \frac{\Delta E}{A_0}\left[J/m^2\right] \tag{1}$$

where ΔE is the energy absorbed till $F=0$ and $A_0 = b(h_{specimen} - h_{notch})$, the initial cross section of the specimen at the notch tip.

Fig. 4 presents an example of test recording on CEAST 9340 machine for PA6.

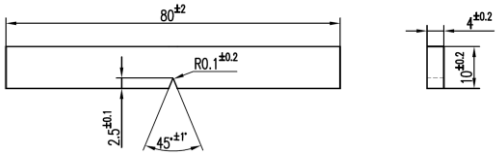

Fig. 2. Specimen dimensions

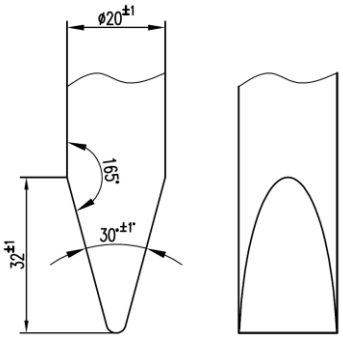

Fig. 3. Impactor geometry

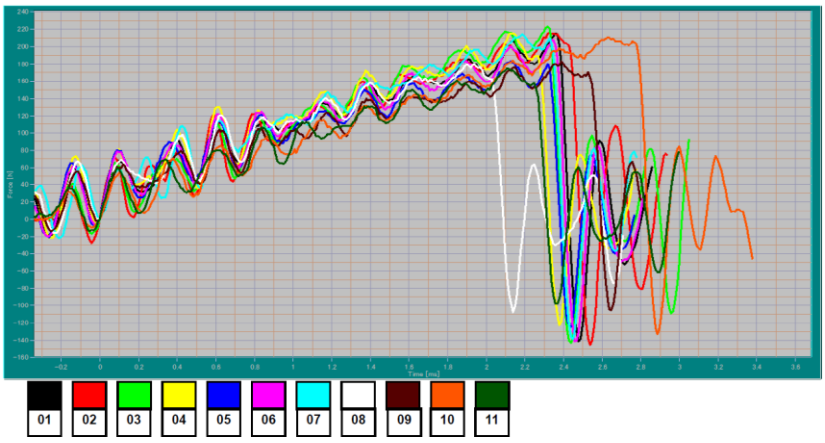

Fig. 4. Example of test recording on CEAST 9340 machine for PA6 (test 10 was excluded) (Materials Strength Laboratory at "Politehnica" University of Bucharest)

3. Discussion on simulation results

For PP, the force-time curve has an evolution with wide oscillations, on an upward trend (Fig. 5a). The energy absorbed by the specimen is calculated till the lowest value of force *F*, before 0, and this will be called the total Charpy impact energy or the energy at break. The value of the energy absorbed between the last positive value of *F* and *F=0* can be neglected because it has a very low value (values of 10^{-5}...10^{-6} J). The moment of cancellation of the impact force for eight specimens was concentrated in the time interval of 0.89×10^{-3} s to 1.1×10^{-3} s, and for the other two specimens the moment for F=0, appeared much later, namely, for specimen 2 at 1.37×10^{-3} s and for specimen 11 at 1.43×10^{-3} s.

The trend of the curves for the absorbed energy is similar to that presented for the material PA6 (Fig. 5b). In [37], there are given data for typical PP,

2.5...50.4 kJ/m^2 at 23 °C, and in [38] the value of Charpy impact resistance is 6.5 kJ/m^2. The values can only be compared for the same test conditions and the same notch shape. One of the tests was done with v_0=0.96 m/s, the others being performed at v_0=0.95 m/s. The test was considered valid because the speed variation was only 1.052% of the velocity value for the other nine tests.

For PA6, the oscillations of the force in time are more pronounced than for PP and three oscillations can be observed, the first of which is very well outlined for all specimens, which reflects that the failure mechanism in this area of the graph is similar for all specimens. The force oscillation in the middle of the graph is more uneven, reflecting the non-uniformity in section, induced by rare cavitation gaps and/or of the different local crystallinity degree. The graph is followed by a third oscillation of the force with different maximum values. The existence of small peaks after this higher oscillation reflects the failure of fibrils generated after the previous oscillations.

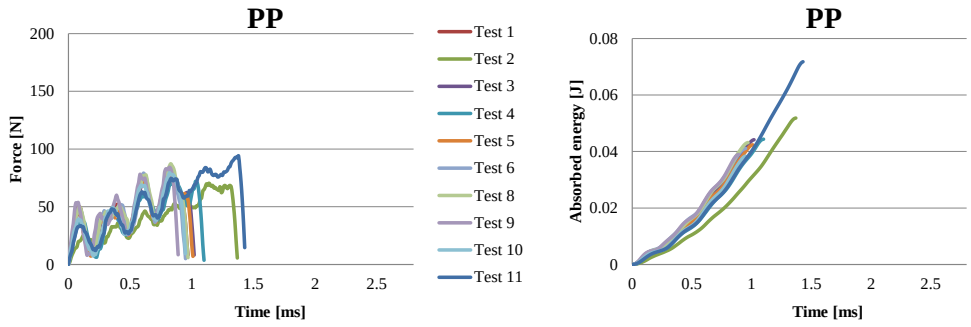

a) Diagram of force and absorbed energy at impact, for material PP

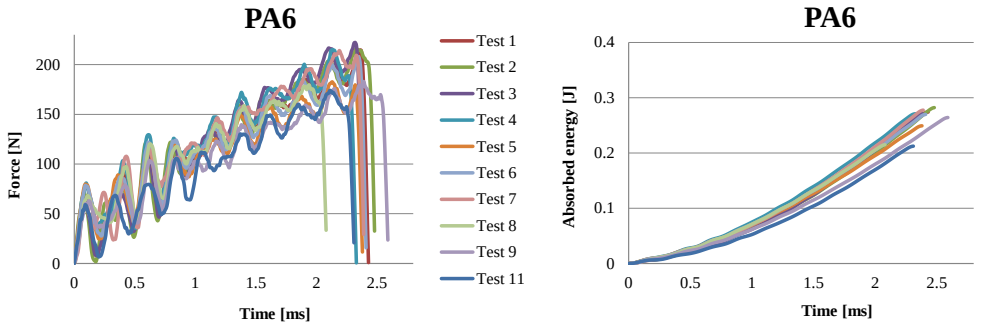

b) Diagram of force and absorbed energy at impact, for material PA6

Fig. 5. Force and absorbed energy curves for the polymer that are the base of the blends

For specimens made of PA6 and for all tests, the values of force-time curve fall in an ascending band with width of about 50 N. Within this band, the tests oscillate with different time periods, shorter at the beginning of the impact and then with longer time periods and oscillations. The tests showed the failure of the

specimens in the range between $t=2.08\times10^{-3}$ s and $t=2.59\times10^{-3}$ s. In contrast, the absorbed energy has a uniform evolution in a relatively small interval; the variation of the absorbed energy for the tested specimens being from 0.21 J to 0.28 J. The energy curve in time has two components, an almost linear area, between $0...1\times10^{-3}$ s and then a curved area until breaking.

For material A (Fig. 6a), the first force peak appears at the moment $t=0.07\times10^{-3}$ s and the first minimum of the force appears at $t=0.18\times10^{-3}$s, after which the specimens have a slightly ascending plateau, followed by a final increasing zone only for two specimens, at $t=0.47\times10^{-3}$ s. For the other eight specimens, a last force maximum was noticed at $t=0.62\times10^{-3}$ s. The force reached zero in the interval $t=0.45...0.84\times10^{-3}$ s. Material A shows three distinct zones on force-time graphs:

- zone I - a curve with a maximum force of 42...55 N and a descent around $t=0.18\times10^{-3}$ s for all tested specimens;
- zone II comprises a sudden rise, a slightly ascending trend and an oscillation with a maximum between 50...82 N; this differs in duration and shape;
- zone III represents the last oscillation of the force, the maximum being between 62...95 N, after which the graph drops to 0.

If the first stage is similar for all specimens, this does not happen for the other zones, the latter differ especially in duration. The oscillations of the force for material A shows that this is a blend and it has zones (volumes) more resistant to break (predominant with PA6, in a higher local concentration) and, therefore, more irregular shapes of the curves appear as compared to PP. The energy at break evolves almost linearly for all specimens, with very small ripples, but the scattering of total energy at break values is over a large range (0.677 J).

Material B has similar curves (Fig. 6b) but, unlike material A, all breaks occur after $t=0.7\times10^{-3}$s. The force value range that includes the tests performed for material B is wider, namely 40 N for the first stage, 50 N for the second stage and 60 N for the last stage. Regarding the energy-time curve, the tested specimens were grouped seven on an almost linear curve, but with a smaller slope and three on a curve consisting of two zones, a linear one with a smaller slope, followed by a slightly parabolic one. The force-time curves of the material B show oscillations with shorter and uneven periods than A. The first stage is similar to the other two materials discussed above (PP and A), but the second stage has different oscillations, the curves do not overlap for all specimens. The time till break varies from 1.06×10^{-3} s to 1.63×10^{-3} s.

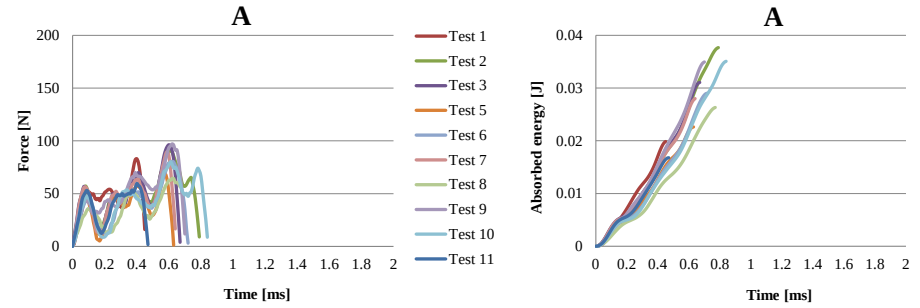

a) Material A

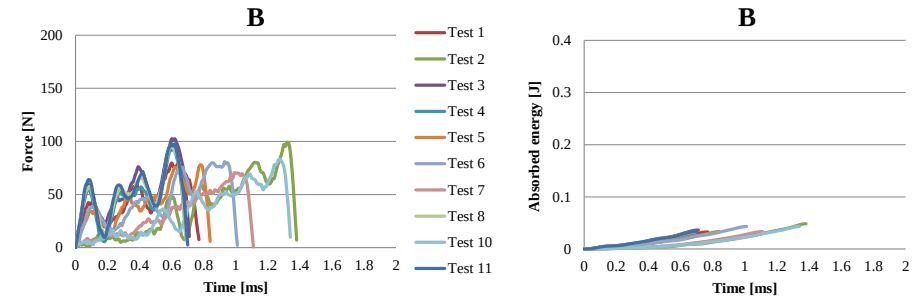

b) Material B

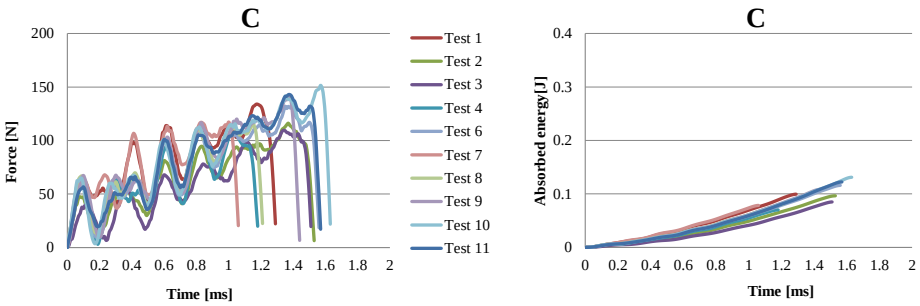

c) Material C

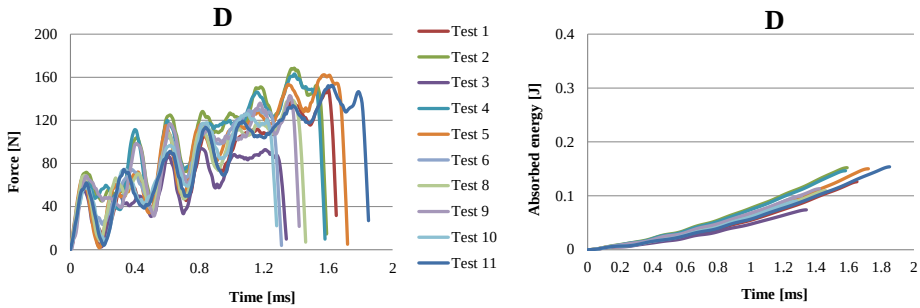

d) Material D

Fig. 6. Evolution in time of force (left) and absorbed energy (right) for the PP+PA6 blends

Material C (Fig. 6c) has energy-time curves with smaller oscillations, but the trend is almost linear, and the scattering range of the results for energy at break is 0.057 J.

Material D (Fig. 6d) has a similar evolution to material C, for all curves analyzed over time (force and absorbed energy). The shape of the absorbed energy-time curve is parabolic and with a smaller radius of curvature, and the variation range of this characteristic is 0.08 J.

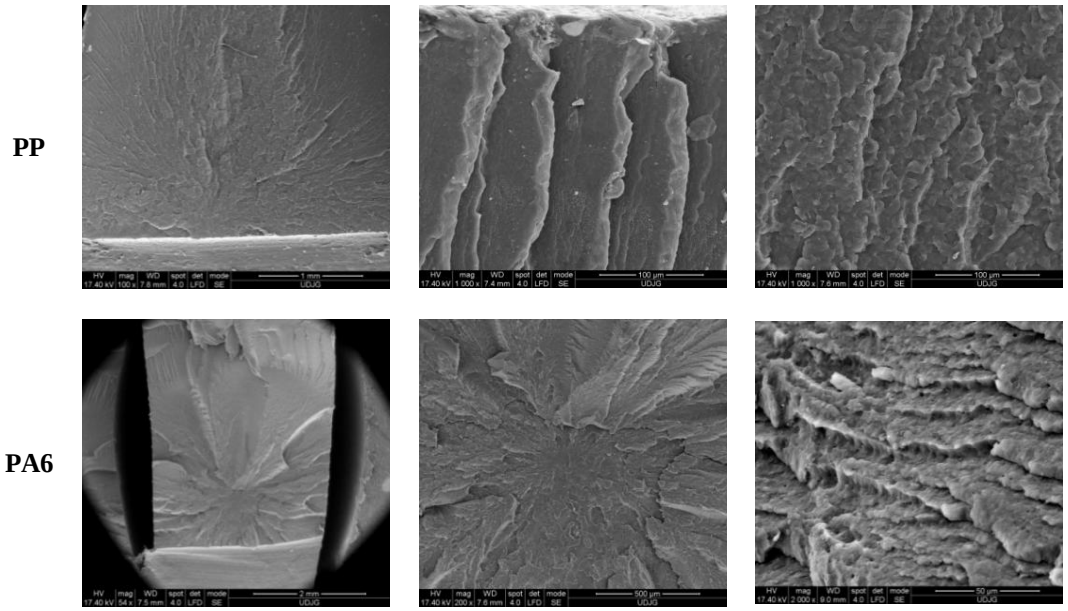

Fig. 7. SEM images for tested materials from the first family,
morphologies of the broken surfaces Charpy PA6 (60 mm distance between supports), v_0=0.96 m/s

Fig. 7 shows morphologies of the broken surfaces, at different scales, obtained by the help of a scanning electron microscope, for the basic polymers (PP and PA6). The SEM images underline the more ductile nature of PA6. Fig. 8 presents SEM images of the blends. Musteata [13] identified the matrix and the droplets in the blends by the help of EDX analysis and concluded that materials A and B had a PP matrix, but materials C and D had a PA6 matrix with PP droplets. First column of images in Fig. 8 includes the view from the notch; images for D in columns 2 and 3 are taken from the side under the impactor, revealing a crushing process due to the more ductile polymer (PA6). Images with higher magnification point out a good dispersion of calcium carbonate and polymer droplets; droplets with crimped coating are the result of polymeric additives (LPDE and Polybond 3200) having an adhesive character that try to diminish the separation of the basic immiscible polymers. Droplets of PA6 are smaller in material A having lower concentration of this component, but at higher concentration (40% wt in material

B), these are larger. Material B has cavitation pores probably generated during specimen molding and cooling, due to the immiscibility of the basic polymers of the blends.

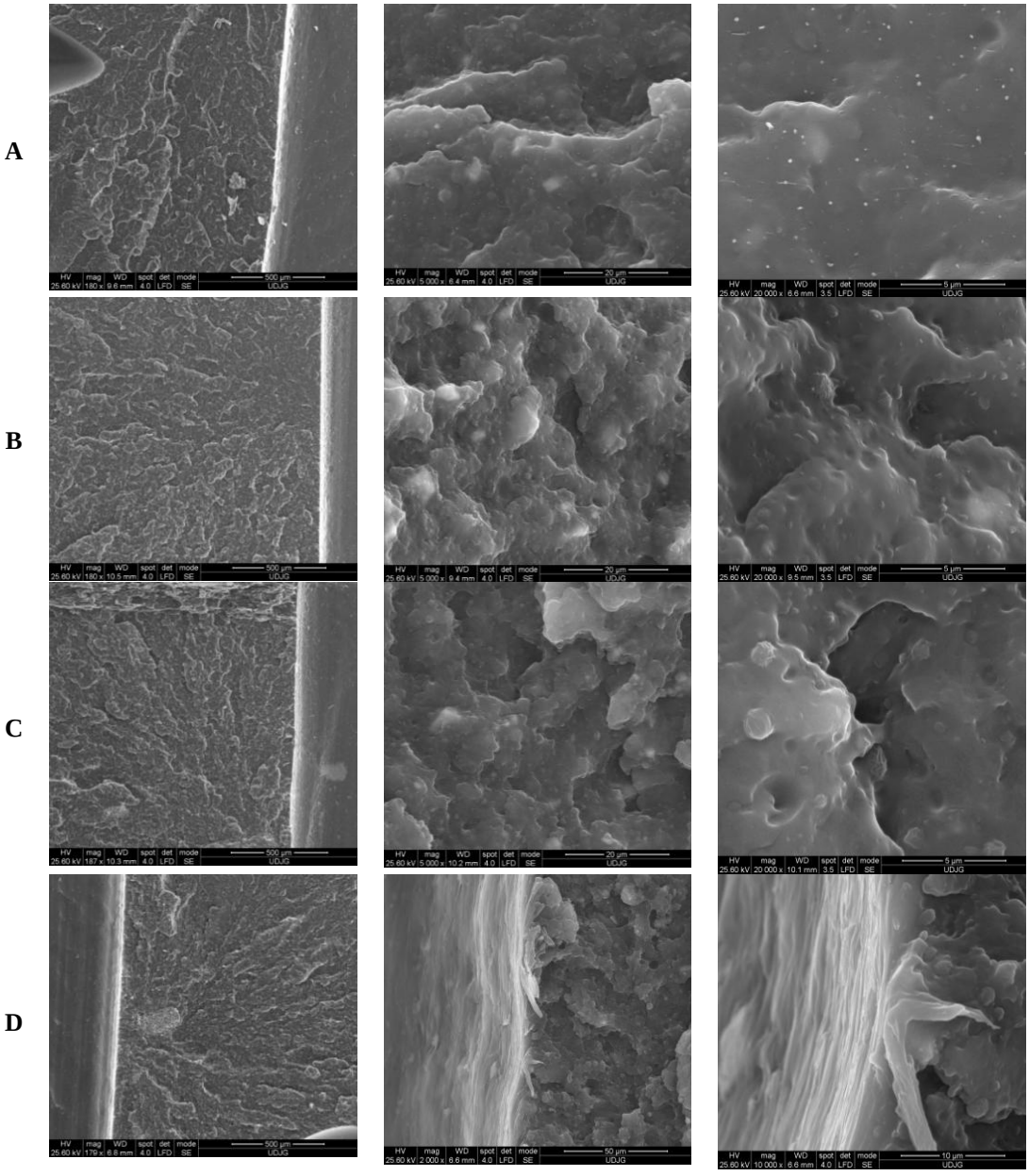

Fig. 8. SEM images for tested materials from the first family

4. Conclusions

The diagram of the average values of the breaking force and their spreading interval (Fig. 9) reveals the following:

- the material that has the lowest maximum force value is PP,
- the material that has the highest maximum force, is PA6,
- blends A, B, C and D have intermediate values for the maximum force, between 81.6 N for PP and 201 N for PA6.

For blends A and B the maximum force is close to that of PP. Increasing the PA concentration leads to an increase in the maximum force for blends C and D, but does not reach the value of polyamide. Scattering intervals increase with increasing PA6 concentration, so the behavior of materials C and D is more difficult to predict. The large scattering for C and D can also be caused by the presence of cavities during molding and cooling the specimens.

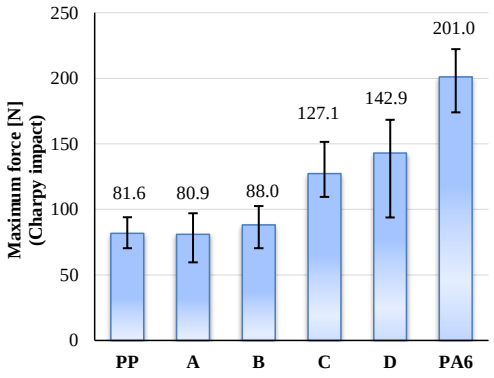

Fig. 9. Average values of maximum force for tested materials

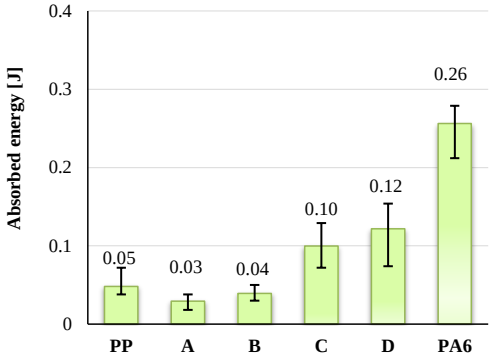

Fig. 10. Average values of absorbed energy at break for tested materials

Fig. 11 shows curves obtained from the average values for these two characteristics, maximum force and absorbed energy till break. Values are given in Table 3 to emphasis the two groups: PP, A and B having lower values and C, D and PA6 with higher values.

Analyzing the results obtained for the tested materials, the conclusions are as follows: there were obtained satisfactory results for energy at break for material C and D, but at half the value of PA6, so the additions in the author's recipes did not substantially improve the impact characteristics, at least up to a speed of 1 m/s.

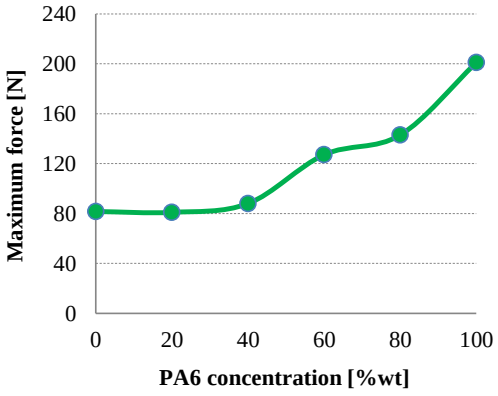

a)

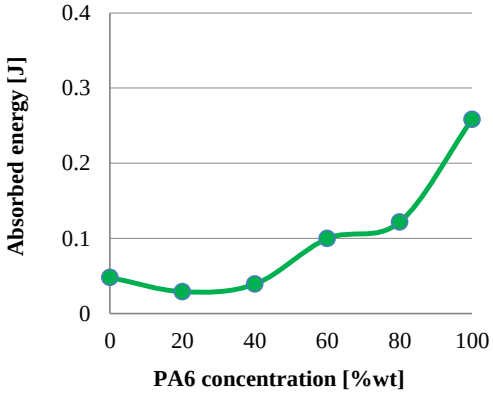

b)

Fig. 11. Average values of force (a) and absorbed energy (b) as a function of PA6 concentration

Table 3

Characteristics obtained from Charpy tests, for the tested materials

Characteristic	PP	A	B	C	D	PA6
Absorbed energy at break [J]	0.048	0.029	0.039	0.09	0.12	0.256
Maximum force [N]	81.61	80.94	87.96	127.14	142.91	200.96
Impact resistance [kJ/m^2] average value range	1.26...2.33 1.603	0.60...1.26 0.96	1.0...1.66 1.29	2.4...4.3 3.32	2.46...5.13 4.05	7.0...9.3 8.52

In addition, blends C and D tend to form cavities due to the immiscibility of the constituent polymers, PA6 and PP, and the modifying agents ($CaCO_3$ and

Polybond 3200) neither eliminate processing problems (especially cavity generation), nor offer an increase energy at break for Charpy tests. Materials C and D should be recommended only they offer other advantages as compared to PA6 and if issues related to cavitation generation will be solved by optimizing the processability.

Acknowledgement

This work is supported by the project ANTREPRENORDOC, in the framework of Human Resources Development Operational Programme 2014-2020, financed from the European Social Fund under the contract number 36355/23.05.2019 HRD OP /380/6/13 – SMIS Code: 123847.

R E F E R E N C E S

[1] *D.V. Rosato and D.V. Rosato*, Plastics Engineered Product Design, Elsevier Ltd, 2003
[2] *D. Rosato, D. Rosato and M. Rosato*, Plastic Product Material and Process Selection Handbook, Elsevier Science & Technology Books, 2004
[3] *M. Boţan, A. E. Musteaţă, T. F. Ionescu, C. Georgescu and L. Deleanu*, Adding aramid fibres to improve tribological characteristics of two polymers, 15th International Conference on Tribology, Kragujevac, Serbia, in Tribology in Industry, **vol. 39**, no. 3, pp. 283-293. http://paper.researchbib.com/view/paper/135458, 2017
[4] *C. Georgescu*, Studii şi cercetări privind evoluţia parametrilor stratului superficial în procesele de frecare şi uzură ale unor materiale compozite cu matrice de polibutilentereftalat (Research on the Evolution of the Superficial Layers in Wear and Friction Processes Involving Composite Materials with Polybutylene Terephthalate) (in Romanian), PhD thesis, "Dunarea de Jos" University of Galati, Romania 2012
[5] *L. A. Utracki*, History of commercial polymer alloys and blends (From a perspective of the patent literature), in Polymer Engineering Science, **vol. 35**, pp. 1–17, 1995
[6] *R. Bradley*, Radiation Technology Handbook, Marcel Dekker, New York, 1984
[7] *M. Biron*, Polypropylene: A chameleon that competes with engineering plastics & many other materials, SpecialChem, https://omnexus.specialchem.com/tech-library/article/polypropylene-a-chameleon-that-competes-with-engineering-plastics-many-other-materials, 2010
[8] *M. C. Grob*, Plastic additives: an answer for the new trends in the plastic industry, BASF Schweiz AG, Tagung Kunststofftechnologie 2012 (HTA-FR), Fribourg, Switzerland, 2012
[9] *J. K Palacios., A Sangroniz., J. I Eguiazabal., A. Etxeberria and A. J. Müller*, Tailoring the properties of PP/PA6 nanostructured blends by the addition of nanosilica and compatibilizer agents, in European Polymer Journal, **vol. 85**, pp. 532–552, 2016
[10] *L. A Utracki.* Polymer Blends Handbook, Kluwer Academic Publishers, Dordrecht, London, ISBN 1-4020-1114-8 Set, 2002
[11] *M. J. Folkes, P. S. Hope*, Polymer blends and alloys. Blackie Academic and Professional, London, 1993
[12] *W. Albrecht, H. Fuchs, W. Kittelmann and J. Lünenschloss*, Manufacture, applications, characteristics, testing processes. Weinheim, Wiley-VCH, 2006
[13] *A. E. Musteaţă*, Characterization of Two Families of Polymeric Blends Based on PA6 and PP by Tensile and Charpy Tests (in Romanian), PhD thesis, "Dunărea de Jos" University, Galati, Romania, 2020

[14] *M. Boţan*, Caracterizarea mecanică și tribologică a unei clase de compozite polimerice (Mechanical and Tribological Characterization of a Class of Polymeric Composites) (in Romanian), PhD thesis, "Dunarea de Jos" University of Galați, Romania, 2014
[15] *W. S. Chow, Z. A. Mohd Ishak and J. Karger-Kocsis*, Compatibilizing effect of maleated polypropylene on the properties and morphology of injection molded polyamide 6/ polypropylene/organoclay nanocomposites, in Polymer, **vol. 44**, pp. 7427–7440, *2003*
[16] *B. Ou, D. Li and Y. Liu*, Compatibilizing effect of maleated polypropylene on the mechanical properties of injection molded polypropylene/polyamide 6/functionalized-TiO2 nanocomposites, in Composites Science and Technology, **vol. 69,** pp. 421–426, 2009
[17] *K. R. Sharma*, Polymer Thermodynamics Blends, Copolymers and Reversible Polymerization, CRC Press Taylor & Francis Group, ISBN 13: 978-1-4398-2640-9, 2012
[18] *C. G'Sell, J. M. Hiver and A. Dahoun*, Experimental characterization of deformation damage in solid polymers under tension, and its interrelation with necking, in International Journal of Solids and Structure, **vol. 39**, pp. 3857–3872, 2002
[19] *S. L. Bai, G. T. Wang, J. M. Hiver and C. G'Sell*, Microstructures and mechanical properties of polypropylene/polyamide 6/polyethelene-octene elastomer blends, in Polymer, **vol. 45**, pp. 3063-3071, 2004
[20] *S. Bai, C. G'Sell, J.-M. Hiverc and C. Mathieu*, Polypropylene/polyamide 6/polyethylene-octene elastomer blends. Part 3. Mechanisms of volume dilatation during plastic deformation under uniaxial tension, in Polymer, **vol. 46**, pp. 6437–6446, 2005
[21] *S.-Y. Fu, B. Lauke, R. K.Y. Lid and Y.-W. Mai*, Effects of PA6,6/PP ratio on the mechanical properties of short glass fiber reinforced and rubber-toughened polyamide 6,6/polypropylene blends, in Composites: Part B, **vol. 37**, pp. 182–190, 2006
[22] *L. Alexandrescu, M. Sönmeza, M. Georgescu, A. Niţuică, R. Ficai, R Trusca., D. Gurău and L. Tudoroi*, Polyamide/Polypropylene/graphene oxide nanocomposites with functional compatibilizers. Morpho-structural and physico-mechanical characterization, in Procedia Structural Integrity, **vol. 5**, pp. 675-682, 2017
[23] *S. Banerjee, M. Joshi, A. K. Ghosh*, Investigations on clay dispersion in polypropylene/clay nanocomposites using rheological and microscopic analysis, in Journal of Applied Polymer Science, **vol. 130,** pp. 4464–4473, https://doi.org/10.1002/app.39590, 2013
[24] *Q. Beuguel, J. Ville, J. Crepin-Leblond, P. Mederic, T. Aubry*, Influence of formulation on morphology and rheology of polypropylene/polyamide blends filled with nanoclay mineral particles, in Applied Clay Science, **vol. 147**, pp. 168–175, 2017
[25] *A. Gonzales-Montiel, H. Keskkula, D. R. Paul*, Impact-modified nylon 6/polypropylene blends: 3. Deformation mechanisms. Polymer, 36, 4621–37, 1995
[26] *F. Laoutid, E. Estrada, R. M. Michell, L. Bonnaud, A. J. Müller and P. Dubois*, The influence of nanosilica on the nucleation, crystallization and tensile properties of PP/PC and PP/PA blends, in Polymer, **vol. 54**, pp. 3982-3993, 2013
[27] *C. G'Sell, S.L. Bai and J.M. Hiver*, Polypropylene/polyamide 6/polyethylene-octene elastomer blends. Part 2: volume dilation during plastic deformation under uniaxial tension, in Polymer, **vol. 45,** pp. 5785–5792, 2004
[28] *M. Chanda and S.K.,Roy*, Plastics fundamentals, properties and testing. CRC Press Taylor & Francis Group, 2009
[29] *R. N. Rothon*, Mineral Fillers in Thermoplastics: Filler Manufacture and Characterisation, in Advances in Polymer Science, **vol. 139**, pp. 67-107, Springer Berlin Heidelberg CY - Berlin, 1999
[30] *M. Hancock and R. N. Rothon*, Principle types of particulate fillers. în: Rothon RN (ed) Particulate-filled polymer composites. Longman, Harlow, p. 50, Rapra Technology Limited, 1995

[31] *K. Wang, C. Wang, J. Li, J. Su, Q. Zhang, R. Du and Q. Fu*, Effects of clay on phase morphology and mechanical properties in polyamide&6/EPDM-g-MA/organoclay ternary nanocomposites, in Polymer, **vol. 48**, pp. 2144–2154, doi: 10.1016/j.polymer.2007.01.070, 2007

[32] *J. Bicerano*, Prediction of Polymer Properties, 3rd edition, Marcel Dekker Inc, New York. 2002

[33] *L.W. McKeen*, The effect of temperature and other factors on plastics and elastomers, William Andrew Inc., 2008

[34] *C. Pirvu, A. E. Musteată, G. G. Ojoc and L. Deleanu*, Numerical and Experimental Results on Charpy Tests for Blends Polypropylene+Polyamide+Ethylene Propylene Diene Monomer (PP+ PA+ EPDM), in Materials 13.24 5837, doi: 10.3390/ma13245837, 2020

[35] *M. Arnold*, Instrumented Pendulum Impact Testing for Plastic, testXpo, https://fdocuments.in/document/instrumented-pendulum-impact-testing-for-plastics-impact-testing-102015-mareike.html, 2015

[36] *Y-C. Ahn and D. R. Paul*, Rubber toughening of nylon 6 nanocomposites, in Polymer, **vol. 47**, pp. 2830–2838, doi: 10.1016/j.polymer.2006.02.074, 2006

[37] *** Polypropylene (PP) Typical Properties Generic PP Impact Copolymer, https://plastics.ulprospector.com/generics/39/c/t/polypropylene-pp-properties-processing/sp/26

[38] ***Polypropylene (PP), http://www.irpcmarket.com/upload/document/datasheet-1516693272.pdf